

SUPPORTING INFORMATION

Engineered coiled-coil HIF1 α protein domain mimic

Dustin Britton^a, Olga Katsara^b, Orin Mishkit^{c,d}, Andrew Wang^{a,e,f}, Neelam Pandya^{c,d}, Chengliang Liu^a, Heather Mao^{a,c,d}, Jakub Legocki^a, Sihan Jia^a, Yingxin Xiao^a, Orlando Aristizabal^{c,d}, Deven Paul^a, Yan Deng^g, Robert Schneider^{b,h}, Youssef Z. Wadghiri^{c,d}, and Jin Kim Montclare^{a,c,i,j,k,*}

^a Department of Chemical and Biomolecular Engineering, New York University Tandon School of Engineering, Brooklyn, New York, 11201, USA.

^b Department of Microbiology, New York University School of Medicine, New York, New York, 10016, USA

^c Center for Advanced Imaging Innovation and Research (CAI2R), New York University School of Medicine, New York, New York, 10016, USA

^d Bernard and Irene Schwartz Center for Biomedical Imaging, Department of Radiology, New York University School of Medicine, New York, New York, 10016, USA

^e Department of Biomedical Engineering, State University of New York Downstate Medical Center, Brooklyn, New York, 11203, USA

^f College of Medicine, State University of New York Downstate Medical Center, Brooklyn, New York, 11203, USA

^g Microscopy Laboratory, New York University Langone Health, New York, NY, 10016, USA

^h Department of Radiation Oncology, New York University School of Medicine, New York, New York, 10016, USA

ⁱ Department of Chemistry, New York University, New York, New York, 10012, USA

^j Department of Biomaterials, New York University College of Dentistry, New York, New York, 10010, USA

^k Department of Biomedical Engineering, New York University, New York, NY, 11201, USA

* Corresponding author

Email: montclare@nyu.edu

Supporting Information

Preliminary in vivo fluorescence imaging.

In the initial phase of our investigation, we conducted preliminary work with four TNBC mice, assigning two mice to each experimental group— H-MAP-N and COMPcc as well as a saline (PBS) control. This aimed to assess the *in vivo* feasibility of monitoring the distribution of our biomaterial. The assessment encompassed both *in vivo* and *ex vivo* imaging within a 2-hour timeframe post-injection, utilizing a 100 μ L volume at a concentration of 500 nM of protein measured by BCA assay. In the context of *ex vivo* imaging, primary tumors were surgically excised, and organs were promptly collected for immediate imaging. This comprehensive approach was aimed at examining the real-time distribution and localization of our biomaterial in the living organisms as well as in extracted tissues, providing valuable insights into its behavior and interaction within the biological context. These results indicated the potential for significant differences in the localization of H-MAP-N (**Figure S5**) as well as indicated some potential for autofluorescence likely from tissue attenuation and surrounding tissues/fur.

In vivo fluorescence assessment during whole body imaging using the IVIS scanner did not reveal notable differences (**Figure S6**), likely due to tissue attenuation, interference from circulating blood, and autofluorescence signals from fur and the gut, significant differences in fluorescence signal were evident 30 minutes post-injection following euthanasia.

Supplementary Figures

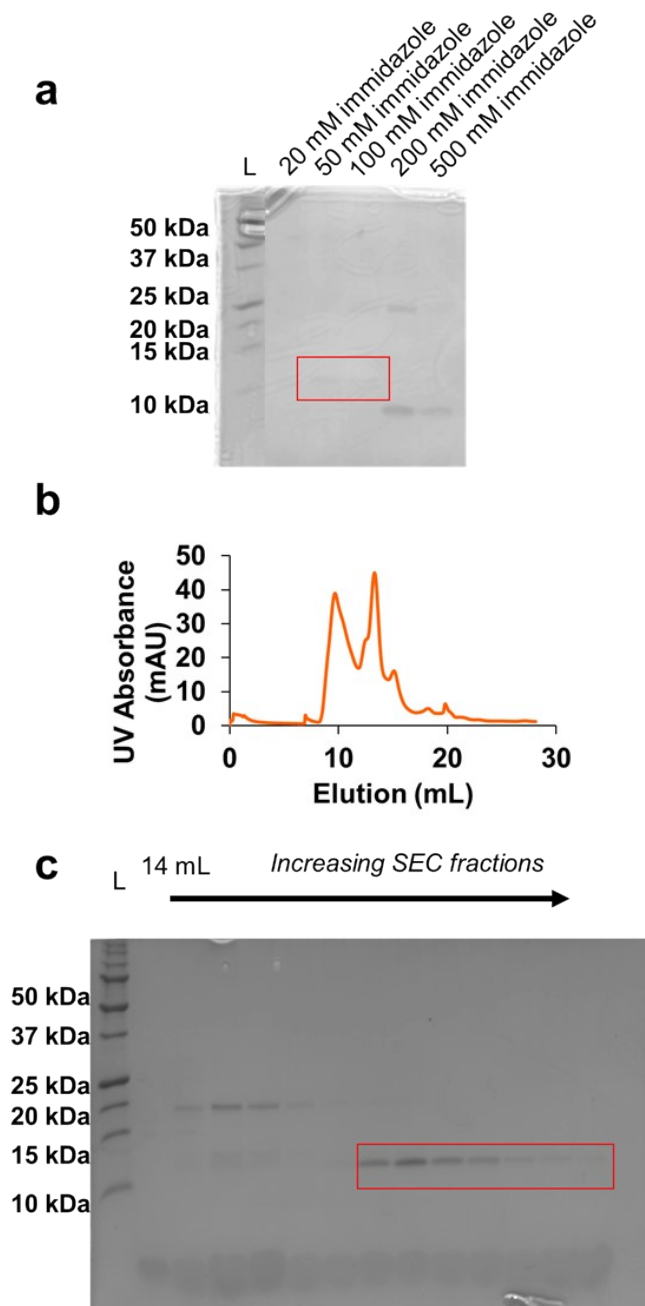


Figure S1 H-MAP biosynthesis workflow showing **a.** 12% SDS-PAGE purification gel following Ni-NTA affinity chromatography (image is cropped for aesthetics and full image is available upon request) and FPLC-SEC with **b.** UV absorbance chromatogram and **c.** corresponding 12% SDS-PAGE gel of collected elutions. Image is cropped for reader

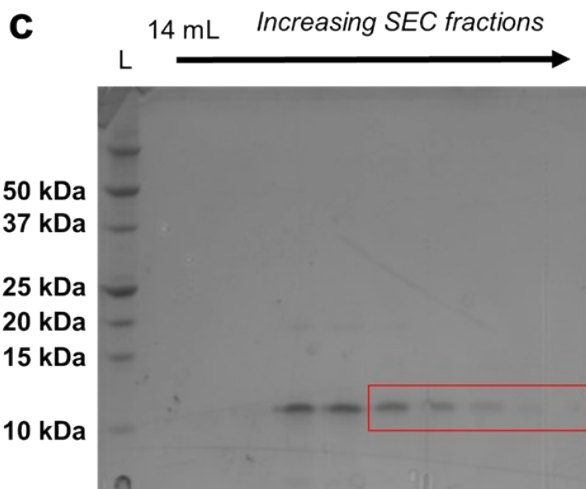
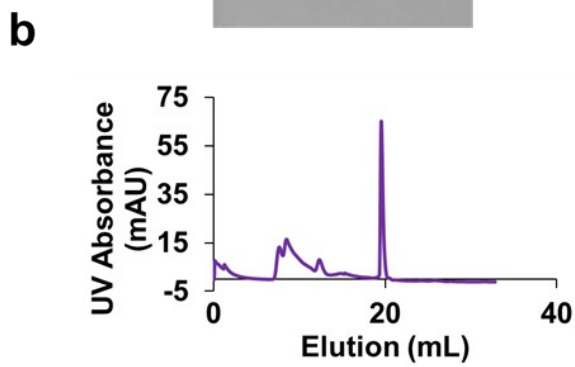
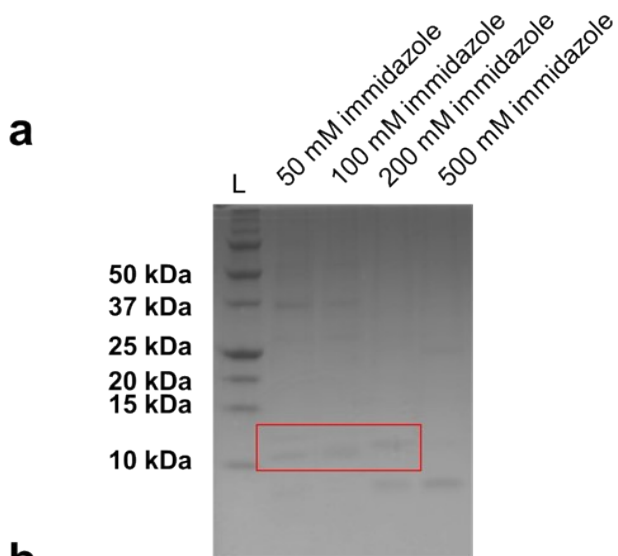


Figure S2 H-MAP-N biosynthesis workflow showing **a.** 12% SDS-PAGE purification gel following Ni-NTA affinity chromatography and FPLC-SEC with **b.** UV absorbance chromatograph and **c.** corresponding 12% SDS-PAGE gel of collected elutions.

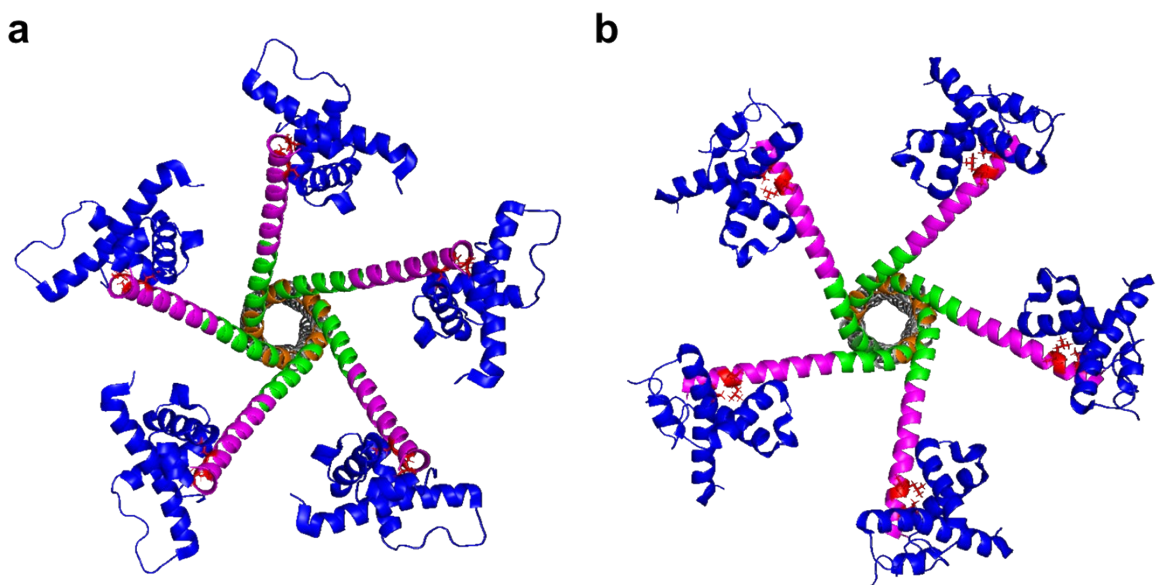


Figure S3 Bird's-eye view of H-MAPs modeled with **a.** the original linker design derived from ACE-MAP and **b.** the new linker design (color-coding matched to **Figure 1**) in complex with p300 (blue) demonstrating sufficient solvent exposure and separation from other multivalent binding arms to allow for available binding in each arm.

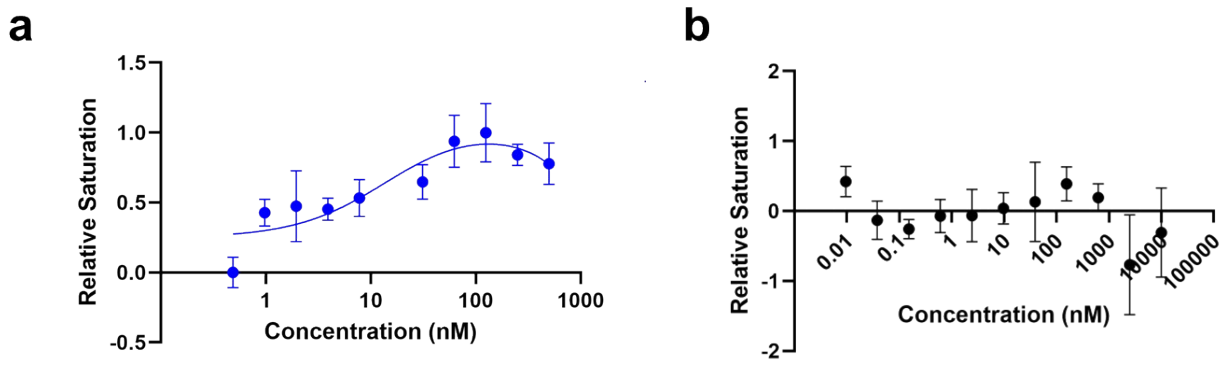


Figure S4 Binding of **a.** HIF1 $\alpha_{786-826}$ and **b.** COMPcc to p300 measured by ELISA where error bars represent the standard deviation of three independent trials.

1.5
1.0
0.5
0.0

Figure S5 Average luciferase activity in relative luminescence units (RLU) under hypoxic and normoxic conditions after incubation of 0-100 nM COMPcc with Luc-MDA-MB-231 cells with hypoxia-inducible luciferase genes. Standard deviation is the result of three independent trials.

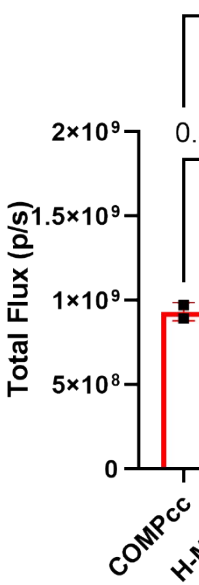


Figure S6 Average total flux (p/s) of preliminary study using two mice each for injection of COMPcc and H-MAP-N and one mouse using saline (PBS) treatment for ex vivo tumor assessment in IVIS using 630/680 ex/em.

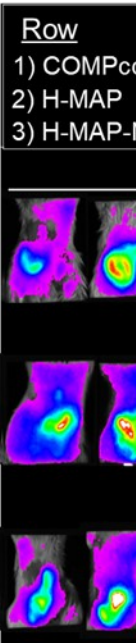
a**b**

Figure S7 in vivo IVIS imaging of mice before (baseline) and 30 min after (post-injection) treatment of COMPcc, H-MAP, and H-MAP-N. **a.** Images show the tumor fluorescence of each group at 630/680 excitation/emission wavelengths. Regions of interest (ROIs) were drawn around the the tumor sites. **b.** Bar graph represents the percentage difference in tumor fluorescence from baseline, reported as total flux (photon per second, p/s). **c.** Bar graph represents the percentage difference in tumor fluorescence from baseline, reported as average radiance (photons per second per square centimeter per steradian, p/s/cm²/sr). **Error bars:** Standard deviation of five independent trials. **Pairwise p-values:** Noted between groups for both total flux and average radiance comparisons.

Supplementary Tables

Table S1. Circular dichroism compositional analysis of H-MAP and H-MAP-N in PBS, pH 7.4. Average and standard deviation from three independent trials of secondary structure content using CONTIN analysis software and mean residue ellipticity from circular dichroism. Average and standard deviation of melting temperature (T_m) is from two independent trials.

	% composition			Mean Residue Ellipticity (Θ) minima (\times deg cm ² dmol ⁻¹)			
	α -helix	β -sheet	Random Coil	$-\Theta_{222}$	$-\Theta_{208}$	$\Theta_{222}/\Theta_{208}$ 8	T_m (°C)
H-MAP	35.8 \pm 10.6	27.2 \pm 5.6	36.7 \pm 4.9	10,000 \pm 2,000	9,400 \pm 2,000	1.0 \pm 0.1	66.6 \pm 0.2
H-MAP-N	35.7 \pm 1.9	29.2 \pm 1.5	34.9 \pm 0.6	9,800 \pm 500	9,300 \pm 900	1.0 \pm 0.1	69.9 \pm 1.7

Table S2. IVIS fluorescence detection at 630/680 excitation/emission of organs *ex vivo*. Average and standard error are the result of four independent trials.

Protein	Total flux of tumor <i>ex vivo</i> ($\times 10^8$ P/s)	Average radiance of tumor <i>ex vivo</i> ($\times 10^7$ P/sec/mm/sq)
H-MAP	7.0 \pm 1.1	5.5 \pm 0.4
H-MAP-N	6.4 \pm 0.7	4.7 \pm 0.3
COMPcc	4.5 \pm 1.1	3.4 \pm 0.4